Article

Stereoselective Association of Binuclear Metallacycles in Coordination Polymers

Andrei N. Khlobystov, Matthew T. Brett, Alexander J. Blake, Neil R. Champness, Peter M. W. Gill, Darragh P. O'Neill, Simon J. Teat, Claire Wilson, and Martin Schrder

J. Am. Chem. Soc., **2003**, 125 (22), 6753-6761• DOI: 10.1021/ja029048y • Publication Date (Web): 10 May 2003

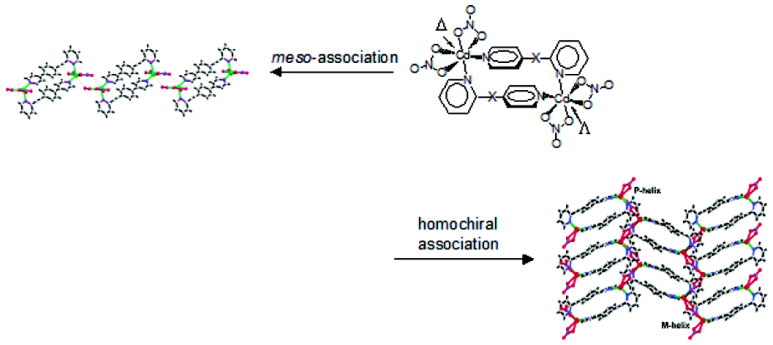

More About This Article

Additional resources and features associated with this article are available within the HTML version:

- Supporting Information
- Links to the 11 articles that cite this article, as of the time of this article download
- Access to high resolution figures
- Links to articles and content related to this article
- Copyright permission to reproduce figures and/or text from this article

View the Full Text HTML

J|A|C|S
ARTICLES
Published on Web 05/10/2003

Stereoselective Association of Binuclear Metallacycles in Coordination Polymers

Andrei N. Khlobystov,[†] Matthew T. Brett,[†] Alexander J. Blake,[†] Neil R. Champness,*[,†] Peter M. W. Gill,[†] Darragh P. O'Neill,[†] Simon J. Teat,[‡] Claire Wilson,[†] and Martin Schröder*[,†]

Contribution from the School of Chemistry, The University of Nottingham, University Park, Nottingham NG7 2RD, U.K., and CLRC Daresbury Laboratory, Daresbury, Warrington, Cheshire WA4 4AD, U.K.

Received October 22, 2002; E-mail: Neil.Champness@nottingham.ac.uk; M.Schroder@nottingham.ac.uk

Abstract: A series of structurally related binuclear metallacycles $[Cd(NO_3)_2L]_2$, where L is an angular *exo*-bidentate ligand, have been synthesized. Each metallacycle contains two coordinatively unsaturated, chiral metal centers within a single molecule, and the assembly of these metallacycles into polymeric framework structures has been studied systematically for the first time. Stereoselective homochiral association of $[Cd(NO_3)_2L]_2$ leads to the formation of helical coordination polymers, whereas *meso* type association results in nonhelical chain structures. The type of stereoselective aggregation depends on the conditions of self-assembly as well as on ligand functionality. Both helical and nonhelical polymeric complexes have been isolated for the metallacycle $[Cd(NO_3)_2(2,4'\text{-pyacph})]_2$ (2,4′-pyacph = 2,4′-(4-ethynylphenyl)bipyridyl). Homochiral association results in the formation of helical $[Cd(NO_3)]_\infty$ chains which link the binuclear $[Cd(NO_3)_2(2,4'\text{-pyacph})]_2$ metallacycles into racemic two-dimensional sheets which contain both *P* and *M* $[Cd(NO_3)]_\infty$ helices. In contrast, *meso*-association leads to the formation of nonhelical one-dimensional chains. It is shown that the product of homochiral association is predominately formed at room temperature and that of *meso*-association is generated at elevated temperatures. Thus, it may be concluded that the homochiral association appears to be energetically less favorable than the *meso*-association, a conclusion that has been confirmed by theoretical calculations of the crystal lattice energy. Several high-yield syntheses of bipyridyl-type ligands used for metallacyclic assembly are also reported.

Introduction

The observation of topological similarities between helical biological molecules and synthetic metal-containing helices based on coordination interactions has stimulated extensive interest in helicates and related chiral topologies.[1,2] Helicity is perhaps the most important structural characteristic of a helicate and may be deduced from the absolute configuration of the component metal.[2] Thus, for the simplest binuclear systems the same absolute configuration, Δ/Δ or Λ/Λ, at both metal centers leads to a P or M helical arrangement of strands, respectively. In contrast, when the two metal centers possess opposing absolute configurations (Δ/Λ), no helical volume is generated, resulting in a nonhelical, centrosymmetric molecule. This simple analysis may be applied to various types of complex[2] and affords a reliable method of interpreting helicity in discrete supermolecules.

The same logic may be extended to metal coordination framework polymers. As for discrete helicates, the infinite chain has a helical conformation[3] when all metal centers within the chain have the same configuration (Scheme 1a).[4,5] In coordination polymers in which both Λ and Δ centers are included in a single chain in equal proportion the conformation of the polymer is achiral and is commonly denoted as a *zigzag* arrangement (Scheme 1b).[6] Elegant experiments comparing the assembly of enantiomerically pure monomeric blocks with their racemic counterparts clearly demonstrate[7] the direct dependence of the

[†] The University of Nottingham.
[‡] CLRC Daresbury Laboratory.

(1) Lehn, J.-M.; Rigault, A.; Siegel, J.; Harrowfield, J.; Chevrier, B.; Moras, D. *Proc. Natl. Acad. Sci. U.S.A.* **1987**, *84*, 2565.
(2) Piguet, C.; Bernardinelli, G.; Hopfgartner, G. *Chem. Rev.* **1997**, *97*, 2005.
(3) Generally speaking, a helix is a figure generated by a motion around and along a line. This implies that any helix can possess only a screw axis as a symmetry element. The presence of other symmetry elements (e.g., inversion centers, mirror planes) within a one-dimensional chain indicates a nonhelical (zigzag) conformation.
(4) Helicity of coordination polymers induced by chiral ligands: (a) Modder, J. F. ; van Koten, G.; Vrieze, K.; Spek, A. *Angew. Chem., Int. Ed. Engl.* **1989**, *28*, 1698. (b) Evans, D. A.; Woerpel, K. A.; Scott, M. J. *Angew. Chem., Int. Ed. Engl.* **1992**, *31*, 430. (c) Suzuki, T.; Kotsuki, H.; Isobe, K.; Moriya, N.; Nakagawa, Y.; Ochi, M. *Inorg. Chem.* **1995**, *34*, 530. (d) Bowyer, P. K.; Porter, K. A.; Rae, A. D.; Willis, A. C.; Wild, S. B. *Chem. Commun.* **1998**, 1153. von Zelewsky, A.; Mamula, O. *J. Chem. Soc., Dalton Trans.* **2000**, 219.
(5) Helicity of coordination polymers induced by chiral metal centers: (a) Caneschi, A.; Gatteshi, D.; Rey, P.; Sessoli, R. *Inorg. Chem.* **1991**, *30*, 3936. (b) Batten, S. R.; Hoskins, B. F.; Robson, R. *Angew. Chem., Int. Ed. Engl.* **1997**, *36*, 636. (c) Biradha, K.; Seward, C.; Zaworotko, M. J. *Angew. Chem., Int. Ed.* **1999**, *38*, 492. (d) Konno, T.; Tokuda, K.; Okamoto, K.; Hirotsu, M.; *Chem. Lett.* **2000**, 1258. (e) Konno, T.; Yoshimura, T.; Aoki, K.; Okamoto, K.; Hirotsu, M. *Angew. Chem., Int. Ed.* **2001**, *40*, 1765.
(6) For example: (a) Ezuhara, T.; Endo, K.; Aoyama, Y. *J. Am. Chem. Soc.* **1999**, *121*, 3279. (b) Ellis, W. W.; Schmitz, M.; Arif, A. A.; Stang, P. J. *Inorg. Chem.* **2000**, *39*, 2547.

Scheme 1. Schematic Representation of (a) a Helical and (b) a Zigzag Coordination Chain

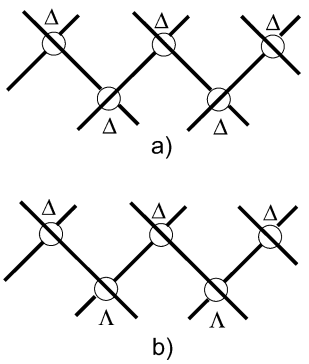

Scheme 2. Schematic Representation of a Coordinatively Unsaturated Binuclear Metallacycle

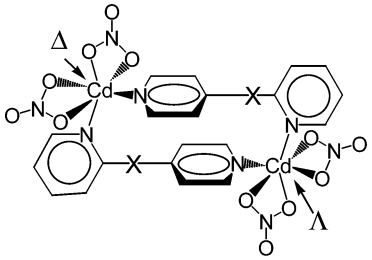

Scheme 3. Angular Ligands Used for Synthesis of $Cd(NO_3)_2$ Binuclear Metallacycles

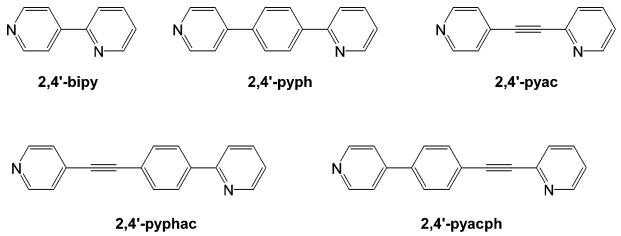

polymeric helicity upon the chirality of the monomeric units within the chain.

All examples of stereoselective noncovalent polymerization reported so far have utilized mononuclear complexes as monomeric building units. However, the structural complexity of the monomeric blocks employed in and for crystal engineering is gradually increasing,[8] and this prompted us to study, for the first time, the stereochemistry of aggregation of *binuclear* metallacycles $[Cd(NO_3)_2L]_2$ (Scheme 2). These metallacycles possess a higher degree of supramolecular complexity by containing two chiral metal centers with opposing absolute configurations (Δ and Λ) related by an inversion center (Scheme 2).

Geometry and Synthesis of Ligands. Angular 2,4′-bipyridyl ligands with a bite angle of 60° (Scheme 3) have been chosen for the assembly of binuclear complexes (Scheme 2). Because of the rigid nature of the spacers between pyridyl rings, the only conformational freedom allowed involves rotation of the aromatic rings about the long axis of the molecule. As a result,

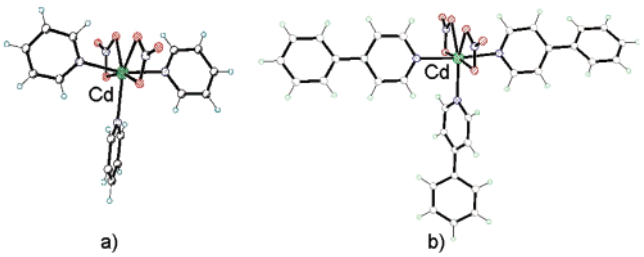

Figure 1. Molecular structure of cadmium nitrate complexes with (a) pyridine[11] and (b) 4-phenylpyridine **1**.

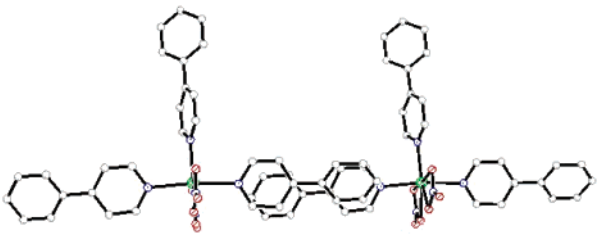

Figure 2. Intermolecular aromatic interactions in the complex $[Cd(NO_3)_2(4\text{-phpy})_3]$, **1**.

these angular ligands exhibit a strong tendency to form cyclic species with various transition metal ions.[9] Metal centers with trigonal, trigonal bipyramidal, and distorted tetrahedral geometries would be expected to form binuclear complexes with this type of ligand, as the match of their geometric parameters is highly conducive to the formation of metallacycles (Scheme 2) where the N−M−N angle is expected to be close to 120°. However, transition metal cations with a flexible coordination geometry such as Cd(II) can potentially adapt the metallacyclic structures.

All ligands were synthesized by cross-coupling reactions in the presence of a palladium complex as catalyst, except 2,4′-pyph, which was prepared according to the literature method[10] involving free radical aromatic substitution on a pyridine ring. Coupling of arylhalides with ethynylpyridines (Scheme 4b−d) was carried out under typical Heck reaction conditions, where amines were used as a base and as a solvent. Use of diisopropylamine in the first step of the synthesis of 2,4′-pyphac (Scheme 4d) is very important, as this amine affords a highly selective and almost quantitative substitution of the iodo group with 4-ethynylpyridine. Alkyl esters of arylboronic acids were used as precursors for coupling of two aryl rings (Scheme 4a,d), although these Suzuki coupling reactions require a stronger inorganic base, a higher temperature, and a more effective catalyst, $[Pd(PPh_3)_4]$, than the corresponding Heck reaction. All ligands were isolated using column chromatography and purified by recrystallization (see Experimental Section).

Coordination Geometry of Complexes with Cadmium Nitrate. A consideration of the geometry of Cd(II) complexes with monodentate pyridyl ligands may assist in the understanding of the structural behavior of the metal cation in metallacycles. The structures of $[Cd(NO_3)_2L_3]$ [L = pyridine,[11] 4-phenylpyridine (4-phpy) **1**] are closely related (Figure 1) to the seven-coordinate Cd(II) centers exhibiting distorted pentagonal bipyramidal geometries, with both chelating nitrates and

(7) (a) Saalfrank, R. W.; Maid, H.; Hampel, F.; Peters, K. *Eur. J. Inorg. Chem.* **1999**, 1859. (b) Shii, Y.; Motoda, Y.; Matsuo, T.; Kai, F.; Nakashima, T.; Tuchagues, J. P.; Matsumoto, N. *Inorg. Chem.* **1999**, *38*, 3519. (c) Chen, J.; MacDonnell, F. M. *Chem. Commun.* **1999**, 2529.
(8) (a) Fyfe, M. C. T.; Stoddart, J. F. *Acc. Chem. Res.* **1997**, *30*, 393. (b) Lehn, J.-M. *Chem. Eur. J.* **1999**, *5*, 2455.
(9) Khlobystov, A. N. Ph.D. Thesis, University of Nottingham, 2002.
(10) Didenko, S. I.; Akimenko, L. V. *Zh. Org. Khim.* **1987**, *23*, 157.
(11) Cameron, A. F.; Taylor, D.; Nuttall, R. H. *J. Chem. Soc., Dalton Trans.* **1972**, 1608.

Scheme 4. Ligand Syntheses

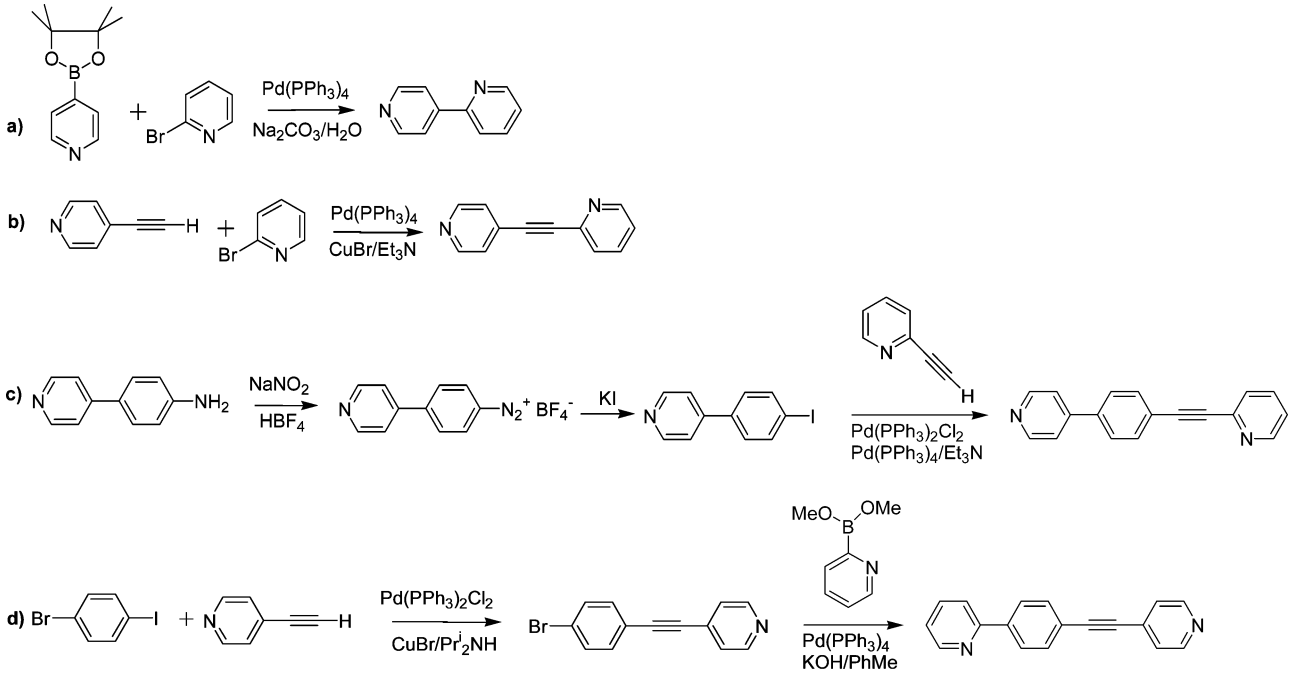

one of the N-donors positioned within the equatorial plane (mean deviation from the plane is 0.061 Å in complex **1**). Cd(II) often adopts T-shaped geometries when combined with *exo*-bidentate linear ligands, giving rise to infinite ladder,[12] herringbone,[12b] or brick-wall[13] type polymers. The flexibility of the Cd(II) coordination polyhedron may, therefore, be highly advantageous for the synthesis of metallacycles. It appears that the T-shaped arrangement of N-donors can adopt other geometries depending on the geometric requirements of the ligand and the conditions of the synthesis. However, regardless of the spatial orientation of the donors, all the Cd(II) centers in the metallacycles described here are seven-coordinate.

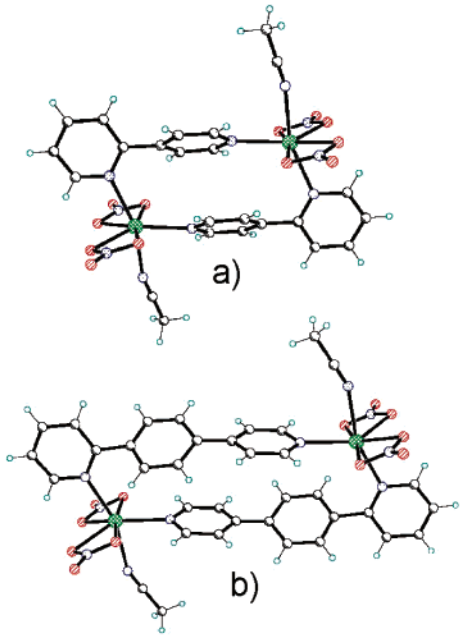

Figure 3. Molecular structures of the metallacycles (a) $[Cd(NO_3)_2(2,4'\text{-bipy})(MeCN)]_2$ **2** and (b) $Cd(NO_3)_2(2,4'\text{-pyph})(MeCN)]_2$ **3**. Each metallacycle has an inversion center.

The crystal structure of $[Cd(NO_3)_2(4\text{-phpy})_3]$ (**1**) displays a packing arrangement where pyridyl rings overlap with phenyl rings (Figure 2). Although in the case of **1** the intermolecular aromatic interaction is not a particularly close one (the centroid−centroid separation of the overlapping rings is over 4 Å), it becomes an important intramolecular contact in the metallacyclic structures (Scheme 2).

Structures of Discrete Metallacycles. The metallacycles $[Cd(NO_3)_2(2,4'\text{-bipy})(MeCN)]_2$ (**2**) and $[Cd(NO_3)_2(2,4'\text{-pyph})(MeCN)]_2$ (**3**) were prepared by reaction of an equimolar mixture of $Cd(NO_3)_2$ with the corresponding ligand, the products crystallizing from a mixture of CH_2Cl_2/MeCN as solvates of MeCN (Figure 3). It is interesting to note that the distorted pentagonal bipyramidal geometry of Cd(II) observed in $[Cd(NO_3)_2py_3]$ is preserved in the binuclear metallacycles: both NO_3^- groups are essentially coplanar and together with the 4-pyridyl group of the ligand occupy the equatorial plane at the metal center. A molecule of MeCN is coordinated in the axial position, completing seven-coordination at the Cd(II) center (Figure 3).

The complex $[Cd(NO_3)_2(2,4'\text{-pyac})(DMF)]_2$ (**4**) prepared by reaction of $Cd(NO_3)_2$ with 2,4′-pyac crystallizes from MeCN/

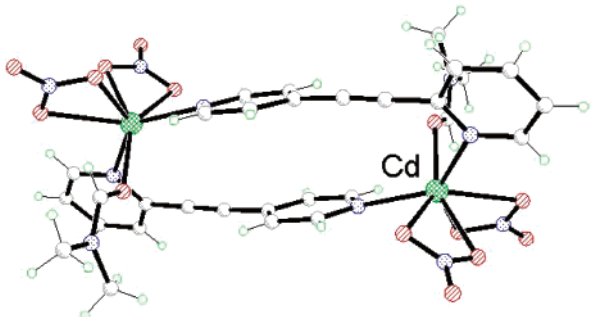

Figure 4. Molecular structure of the complex $[Cd(NO_3)_2(2,4'\text{-pyac})(DMF)]_2$, **4**

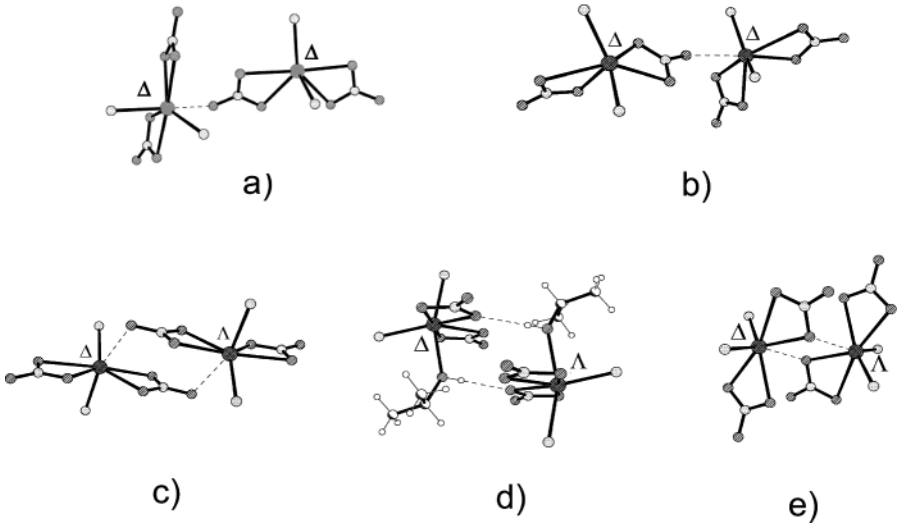

Figure 5. Bridging modes of NO_3^- groups between two metallacycles observed in the complexes (a) $\{[Cd(NO_3)_2(2,4'\text{-pyph})]_2\}_\infty$,[15] (b) β-$\{[Cd(NO_3)_2(2,4'\text{-pyacph})]_2\}_\infty$, **5** (homochiral modes), (c) α-$\{[Cd(NO_3)_2(2,4'\text{-pyacph})]_2\}_\infty$, **6**, (d) $\{[Cd(NO_3)_2(2,4'\text{-pyacph})(Pr^iOH)]_2\}_\infty$, **7**, and (e) $\{[Cd(NO_3)_2(2,4'\text{-pyphac})]_2\}_\infty$, **8** (*meso*-modes).

DMF and has an alternative arrangement of donors around the Cd(II) cation. As in the complexes **1**−**3**, the Cd(II) center in $[Cd(NO_3)_2(2,4'\text{-pyac})(DMF)]_2$ (**4**) is seven-coordinate, but NO_3^- groups in **4** are not coplanar, resulting in an irregular coordination geometry at the metal centers (Figure 4). Despite the difference in the arrangement of the NO_3^- groups in complexes **2**−**4**, all the metallacycles have similar geometries, allowing intramolecular aromatic interaction between overlapping pyridyl and phenyl rings of the ligand, with interplanar separations in the range 3.3−3.5 Å.[14] This attractive interaction favors the formation of metallacycles over acyclic polymeric structures.

***Meso* versus Homochiral Association of Metallacycles in Polymeric Arrays.** The metallacycles $[Cd(NO_3)_2L]_2$ (L = 2,4′-pyacph, 2,4′-pyphac) are coordinatively unsaturated and in the absence of coordinating solvents interact with each other via bridging nitrate units (Figure 5) to form infinite coordination framework polymers.[15] The structural flexibility of bridging NO_3^- groups, which can adopt several coordination modes, in conjunction with the stereochemical arrangement of moieties $[Cd(NO_3)_2L]_2$ containing two chiral metal centers, makes them versatile building blocks for the construction of infinite structures. Two distinct coordination modes of the bridging NO_3^- [μ^1-O^1, O^2 (Figure 5a−c) and μ^2-O^1, O^2 (Figure 5d,e)] can be identified in the polymeric structures of $[Cd(NO_3)_2L]_2$. Such metallacycles can, in principle, link to allow two possible stereochemical interactions: homochiral interactions (Figure 5a,b) when centers of the same configuration (i.e., all Δ or all Λ) are linked together, or *meso* type interactions (Figure 5c−e) when centers of opposing configuration are bound. The impact of stereochemical recognition is perhaps most pronounced for the metallacycle $[Cd(NO_3)_2(2,4'\text{-pyacph})]_2$ (Scheme 2).

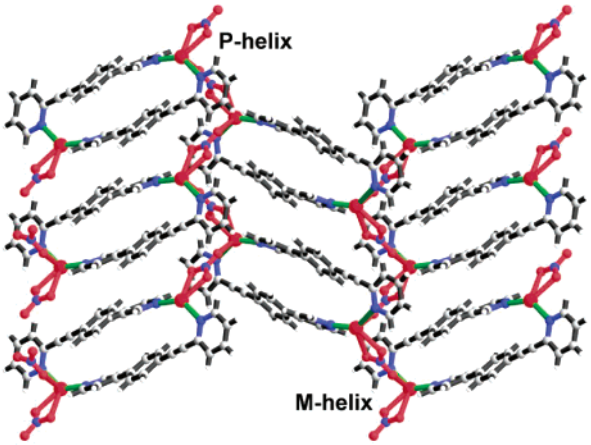

Figure 6. Helical arrangement of the metallacycles $[Cd(NO_3)_2(2,4'\text{-pyacph})]_2$ in the β-polymorph **5** illustrating the homochiral association within each $[Cd(NO_3)]_\infty$ chain. Spontaneous resolution of Δ and Λ centers generates two types of 2-fold helices, *P* and *M*.

Reaction of 2,4′-pyacph with $Cd(NO_3)_2$ in $MeCN/CH_2Cl_2$ affords the complex $[Cd(NO_3)_2(2,4'\text{-pyacph})]_2$, which can be arranged in two different ways to give coordination polymer **5** (Figure 6) or **6** (Figure 7), depending on the specific reaction conditions used. Single-crystal X-ray diffraction studies confirm the structural arrangements, and the phase purity of the polymers was confirmed by powder X-ray diffraction, with **5** having an additional molecule of MeCN in the crystal lattice.

At room temperature the metallacycles $[Cd(NO_3)_2(2,4'\text{-pyacph})]_2$ assemble in a homochiral fashion to give **5**, in which Cd(II) centers are linked by NO_3^- groups (Figure 5b) to form enantiomerically pure $[Cd(NO_3)]_\infty$ coordination chains which adopt a helical conformation (Figure 6). Due to the spontaneous resolution of Δ and Λ centers in **5**, there are two types of 2-fold helices, *P* and *M*, respectively, each arranged around a crystallographic 2_1 screw axis (Figure 6). Each metallacycle interacts with four others, two at each end of the metallacycle, and is involved in both *M* and *P* helices at opposing ends of the binuclear fragment. Binding of the $[Cd(NO_3)]_\infty$ helices via the metallacyclic units affords a two-dimensional sheet structure

(12) (a) Fujita, M.; Sasaki, O.; Watanabe, K. Y.; Ogura, K.; Yamaguchi, K. *New J. Chem.* **1998**, *22*, 189. (b) Fujita, M.; Kwon, Y. J.; Sasaki, O.; Yamaguchi, K.; Ogura, K. *J. Am. Chem. Soc.* **1995**, *117*, 7287.
(13) Withersby, M. A.; Blake, A. J.; Champness, N. R.; Cooke, P. A.; Hubberstey, P.; Schröder, M. *New J. Chem.* **1999**, *23*, 573.
(14) (a) Hunter, C. A.; Sanders, J. K. M. *J. Am. Chem. Soc.* **1990**, *112*, 5525. (b) Janiak, C. *J. Chem. Soc., Dalton Trans.* **2000**, 3885.
(15) Blake, A. J.; Champness, N. R.; Khlobystov, A. N.; Parsons, S.; Schröder, M. *Angew. Chem., Int. Ed.* **2000**, *39*, 2317.

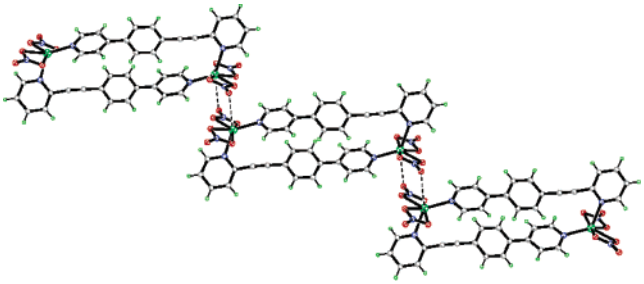

Figure 7. *Meso* arrangement of metallacycles $[Cd(NO_3)_2(2,4'\text{-pyacph})]_2$ in α-polymorph **6**.

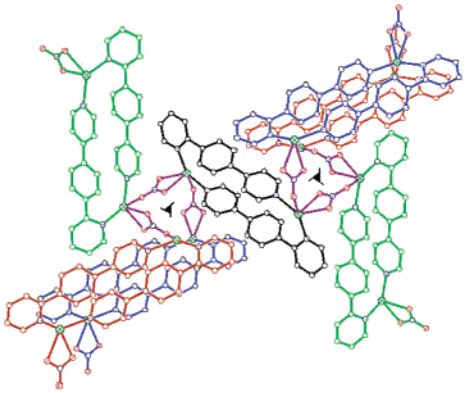

Figure 8. Helical arrangement of metallacycles $[Cd(NO_3)_2(2,4'\text{-pyph})]_2$ forming 3-fold helices.[15]

which contains equal numbers of *P* and *M* helices. Similarly, metallacycles $[Cd(NO_3)_2(2,4'\text{-pyph})]_2$[15] display a mode of homochiral recognition highly related to that observed for $[Cd(NO_3)_2(2,4'\text{-pyacph})]_2$, the only difference being that in $[Cd(NO_3)_2(2,4'\text{-pyph})]_2$, crystallized in the space group *R*-3, the $[Cd(NO_3)]_\infty$ helices are arranged around crystallographic 3_1 or 3_2 screw axes, leading to the formation of a three-dimensional framework structure (Figure 8).

Complex **5** can be irreversibly transformed into its pseudo-polymorph **6** when dispersed in a polar organic solvent, Bu^nOH/*o*-xylene, at elevated temperatures. The product **6** is built of the same binuclear blocks $[Cd(NO_3)_2(2,4'\text{-pyacph})]_2$ linked by NO_3^- groups adopting the same bridging mode as in complex **5**, but these are now linked by *meso* type intermolecular interactions (Figure 5c). Thus each Δ-Cd center is linked through a bridging nitrate group which satisfies the Cd(II) coordination requirements to a Λ-Cd center such that they are related by an inversion center (Figure 5c). As a result of this Δ/Λ pairing of the metal centers, each metallacycle $[Cd(NO_3)_2(2,4'\text{-pyacph})]_2$ interacts with two others, one at each end of the metallacycle: this does not lead to an infinite *helical* array but to a one-dimensional chain consisting of binuclear units in a *meso* arrangement (Figure 7).

Meso supramolecular recognition is also observed for $\{[Cd(NO_3)_2(2,4'\text{-pyacph})(Pr^iOH)]_2\}_\infty$ (**7**), in which one Pr^iOH completes the coordination sphere of each Cd(II) center to give a distorted pentagonal bipyramid (Figure 5d). This leads to the formation of a chain polymer, topologically similar to **6** in which binuclear units $[Cd(NO_3)_2(2,4'\text{-pyacph})(Pr^iOH)]_2$ are linked by O−H···O hydrogen bonds (Figure 5d) in a *meso*-fashion (Figure 9).

A structural isomer of $[Cd(NO_3)_2(2,4'\text{-pyacph})]_2$, metallacycle $[Cd(NO_3)_2(2,4'\text{-pyphac})]_2$ (**8**), synthesized at elevated temperatures under thermodynamic conditions (120 °C), has also been found to adopt exclusively a *meso* type intermetallacycle interaction (Figure 5e). The chain polymer in **8** has a topology resembling that of polymer **6** but with a different nitrate bridging mode (Figures 5e and 10). Nitrate groups in complex **8** are in a μ_2-O^1, O^2-bridging mode (Figure 5e) linking together two metal centers of opposing chirality, whereas in complex **6** the same type of *meso*-arrangement of metallacyles is provided by nitrate groups in a μ_1-O^1, O^2 bridging mode (Figure 5c)

However, unlike its structural isomer 2,4′-pyacph, the ligand 2,4′-pyphac (Scheme 3) can also form a mononuclear complex $[Cd(NO_3)_2(2,4'\text{-pyphac})_2(H_2O)]$ (**9**) when the reaction between the relevant starting materials is performed at room temperature. Despite a reaction M:L stoichiometry of 1:1, the product adopts a 1:2 M:L ratio and the metal center is coordinated only by the more accessible 4-pyridyl donors while the 2-pyridyls remain uncoordinated. The mononuclear $[Cd(NO_3)_2(2,4'\text{-pyphac})_2(H_2O)]$ units are arranged in a polar polymeric chain via the bridging NO_3^- groups (Figure 11). Unlike the metallacycles **2**−**8** with seven-coordinate Cd(II), metal centers in complex **9** are six-coordinate, adopting a distorted octahedral geometry. Both nitrate groups in **9** are monodentate: one of them bridges Cd centers within a coordination chain and another is involved in an intermolecular hydrogen bond with a molecule of water from a neighboring chain. Significantly, complex **9** transforms irreversibly to complex **8** at 120 °C.

Relative Stability of *Meso* (α) and Homochiral (*β*) Forms of $[Cd(NO_3)_2(2,4'\text{-pyacph})]$. Empirical observations demonstrated that homochiral *β*-$\{[Cd(NO_3)_2(2,4'\text{-pyacph})]_2\}$ (**5**) and *meso* α-$\{[Cd(NO_3)_2(2,4'\text{-pyacph})]_2\}$ (**6**), formed from the same components but under different reaction conditions, can be related as kinetic and thermodynamic products, respectively. Thus, it has been shown that **5** is predominately formed at room temperature and **6** is formed at temperatures above 100 °C; moreover, **5** can be irreversibly transformed into **6** at elevated temperatures in polar solvents.

As both complexes **5** and **6** consist of the same building blocks $[Cd(NO_3)_2(2,4'\text{-pyacph})]_2$, they may be regarded as supramolecular isomers differing in the type of association of the monomeric units in the polymeric array. The complexes **5** and **6** have NO_3^- groups in the same type of bridging mode [O^1, μ^1-O^2]: the major difference between them lies in the stereochemistry of the metallacyle−metallacycle interaction, and it is this which is responsible for the difference in their thermodynamic stability.

To estimate the relative stability of the homochiral and the *meso* arrangements, calculations of lattice energies for α-$\{[Cd(NO_3)_2(2,4'\text{-pyacph})]_2\}$ (**6**) and *β*-$\{[Cd(NO_3)_2(2,4'\text{-pyacph})]_2\}$ (**5**) were performed. The lattice energy is defined as the decrease in energy resulting from the aggregation of cadmium dimers $[Cd(NO_3)_2(2,4'\text{-pyacph})]_2$ and is calculated using the following formulas:

$$E_{\beta-\text{form}} = \frac{\frac{1}{2}\left(\sum_i^{4N}\sum_j^{4N} q_i q_j \sum_{\nu\in Z^3}^{\infty}{}' \frac{1}{|\mathbf{d}_i - \mathbf{d}_j + \mathbf{A}\nu|} - 4\sum_i^{N}\sum_j^{N}\frac{q_i q_j}{|\mathbf{d}_i - \mathbf{d}_j|}\right)}{4}$$

$$E_{\alpha-\text{form}} = \frac{1}{2}\left(\sum_i^{N}\sum_j^{N} q_i q_j \sum_{\nu\in Z^3}^{\infty}{}' \frac{1}{|\mathbf{d}_i - \mathbf{d}_j + \mathbf{A}\nu|} - \sum_i^{N}\sum_j^{N}\frac{q_i q_j}{|\mathbf{d}_i - \mathbf{d}_j|}\right)$$

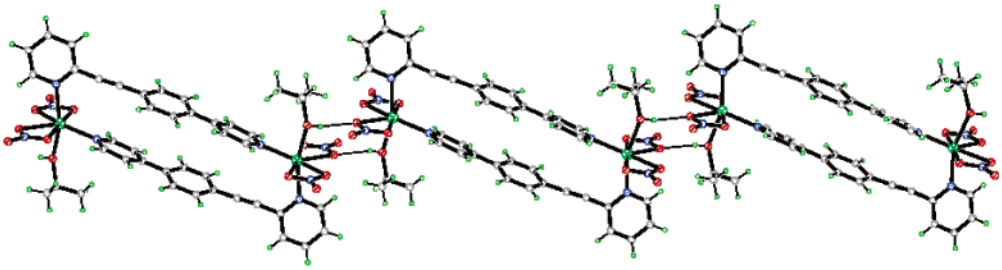

Figure 9. *meso* arrangement of metallacycles $[Cd(NO_3)_2(2,4'\text{-pyacph})(Pr^iOH)]_2$ in chain polymeric complex **7**. Hydrogen bonds are shown as dashed lines.

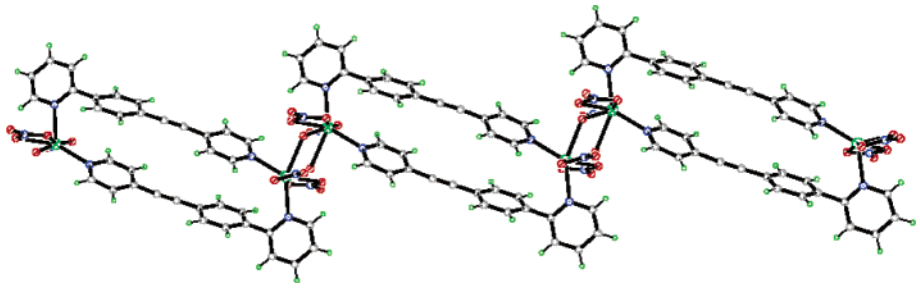

Figure 10. *meso* arrangement of metallacycles $[Cd(NO_3)_2(2,4'\text{-pyphac})]_2$ in chain polymeric complex **8**.

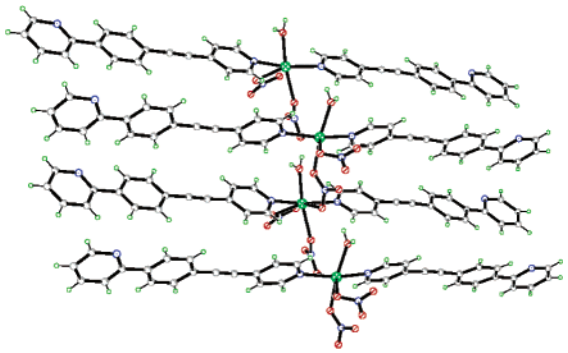

Figure 11. Mononuclear fragments $[Cd(NO_3)_2(2,4'\text{-pyphac})_2(H_2O)]$ arranged in a chain polymer **9**.

where N is the number of atoms in the metallacycle, q_i is the charge and $\mathbf{d}_i$ the position of atom i, $\mathbf{A}$ is a matrix containing the lattice vectors, and $\boldsymbol{v}$ is a vector of integers which replicates the crystal across all space. The prime on the summation indicates that the singularity at (0,0,0) should be avoided so that the sum converges. It should be noted that the two formulas differ in form as the unit cell for the homochiral association product **5** contains four binuclear metallacycles per cell. The first term within the parentheses is a Madelung type sum and is performed using a standard method.[16] The second term removes from this sum the interactions within the metallacycle itself. This method was applied to the two isomers using the Q-Chem 2.0 package[17] to compute Mulliken atomic charges at the B3LYP/SRSC level of theory. The experimental monomer geometries were used. The lattice energy for the homochirally associated β-form **5** was found to be approximately -112 kJ/mol, while a value of -199 kJ/mol was calculated for the *meso*-associated α-form **6**. The lattice energy was also calculated for the mononuclear unit $Cd(2,4'\text{-pyacph})(NO_3)_2$ to ensure that the interaction of the two units to form the metallacycle $[Cd(2,4'\text{-pyacph})(NO_3)_2]_2$ was not significant in determining the thermodynamic product. The results from this calculation showed the β-form **5** to be more stable than indicated by the previous method, and there was no change for α-form **6**. Despite this energy change, product **6** was still clearly the more thermodynamically stable, with $\sim$1.5 times the lattice energy of **5**.

To provide a check of the various methods employed in the above calculation, the lattice energy was also calculated using multipolar interactions. Since the dicadmium unit has a center of inversion, the first nonzero multipole moment is the quadrupole followed by the hexadecapole. Hence, the most significant interaction is the quadrupole−quadrupole interaction, and this decays quickly so it can be summed directly. This predicts the *meso*-associated product **6** to be 1.9 times more stable than the homochirally associated **5**, which is in good agreement with the previous calculation, which predicts a value of 1.8. These results compare the relative stabilities of the homochiral **5** or *meso* arrangement **6** between $[Cd(2,4'\text{-pyacph})(NO_3)_2]_2$ metallacycles rather than the relative stabilities of the final products from the reactions. The final crystalline products observed for **5** and **6** differ in that **5** contains an additional guest MeCN solvent molecule, which can be anticipated to have an influence on the relative stabilities of the two products. However, although the absolute values of the lattice energies computed will not be exact, the relative energies can be used to assign with confidence the nonhelical structure **6** as the thermodynamic product in accordance with the experimental observations.

In summary, we have successfully performed, for the first time, the controlled aggregation of a series of structurally related cyclic supermolecules $[Cd(NO_3)_2L]_2$ whose unique feature is the presence of two coordinatively unsaturated metal centers of opposite chirality within a single molecule. The stereoselective homochiral association of $[Cd(NO_3)_2L]_2$ leads to formation of helical $[Cd(NO_3)]_\infty$ chains within two-dimensional coordination polymers, whereas the *meso* type association results in nonhelical chain structures. It should be noted that unlike previous examples of controlled selective homochiral/hetero-

(16) Crandall, R. E.; Buhlar, J. P. *J. Phys. A* **1987**, *20*, 5497.
(17) Kong, J.; White, C. A.; Krylov, A. I.; Sherrill, C. D.; Adamson, R. D.; Furlani, T. R.; Lee, M. S.; Lee, A. M.; Gwaltney, S. R.; Adams, T. R.; Ochsenfeld, C.; Gilbert, A. T. B.; Kedziora, G. S.; Rassolov, V. A.; Maurice, D. R.; Nair, N.; Shao, Y.; Besley, N. A.; Maslen, P. E.; Dombroski, J. P.; Daschel, H.; Zhang, W.; Korambath, P. P.; Baker, J.; Byrd, E. F. C.; Van Voorhis, T.; Oumi, M.; Hirata, S.; Hsu, C.-P.; Ishikawa, N.; Florian, J.; Warshel, A.; Johnson, B. G.; Gill, P. M. W.; Head-Gordon, M.; Pople, J. A. *J. Comput. Chem.* **2000**, *21*, 1532.

chiral self-assembly,[7] where the type of aggregation depends mostly on the steric and topological requirements of the ligand, in the current case of metallacycles $[Cd(NO_3)_2L]_2$ the stereoselectivity depends on conditions of self-assembly as well as on ligand functionality, and this makes these complexes versatile building blocks for coordination polymer synthesis. The stereoselective recognition observed for these metallacycles $[Cd(NO_3)_2L]_2$ is vital for supramolecular synthesis, as it demonstrates explicitly the effect of enantioselective aggregation on the helicity and overall topology of the polymer. The *meso* type of interaction between monomeric units within the polymeric array appears to be energetically more favorable than the homochiral type, and this is confirmed by theoretical calculations. We are currently continuing our studies toward the rational design of coordination polymers using chiral polynuclear building blocks.

Experimental Section

General Procedures. All reagents (Aldrich) were used as received. The ligand 2,4′-pyph was prepared by the literature method.[10] 4-Ethynylpyridine, 2-ethynylpyridine, dimethyl-2-pyridylboronate, and 4-(4′-aminophenyl)pyridine were prepared using literature methods,[18−21] respectively. 2-(4-Pyridyl)-4,4,5,5-tetramethyl-1,3-dioxaborane and 4-iodopyridine were prepared by the literature method.[21] Elemental analyses (C, H, N) were carried out at the University of Nottingham. Infrared spectra were obtained as KBr pressed pellets using a Perkin-Elmer 1600 series FTIR spectrometer.

Ligand Synthesis. 2,4′-Bipyridine (2,4′-bipy). Aqueous Na_2CO_3 (0.1 g, 0.09 mmol) in deoxygenated water (3 cm^3) and 2(4-pyridyl)-4,4,5,5-tetramethyl-1,3-dioxabororane (0.1 g, 0.5 mmol) were added to a solution of 2-bromopyridine (0.07 g, 0.4 mmol) and $Pd(PPh_3)_4$ (0.002 g, 0.02 mmol) in 5 cm^3 of toluene. The resultant two-layer mixture was stirred and heated at 80 °C for 3 days. An aqueous solution of ammonia (10 cm^3) was added to the reaction mixture. The product was extracted with CH_2Cl_2 (3 × 15 cm^3), and the organic layer was separated and dried over Na_2SO_4. The solvent was then removed in vacuo, and the crude product was purified by column chromatography (toluene/acetone, 3:1, silicagel-60). Yield 40 mg (57%) of viscous yellowish liquid, which slowly crystallizes at −20 °C as a yellow waxy solid. Mp < 30 °C. ^{1}H NMR (DMSO-d_6, ppm): 8.75 (d, 1H), 8.70 (d, 2H), 8.13 (d, 1H), 8.08 (d, 2H), 7.98 (t, 1H), 7.50 (t, 1H). Calc for $C_{10}H_8N_2$: C 79.62, H 5.13, N 17.95. Found: C 78.98, H 5.17, N 17.88. MS (EI, *m*/*z*): 156 $[M]^+$.

2,4′-(1,2-Ethynyl)bipyridine (2,4′-pyac). 2-Bromopyridine (0.3 g, 1.9 mmol), $Pd(PPh_3)_4$ (0.01 g), copper(I) bromide (0.006 g, 0.04 mmol), and 4-ethynylpyridine (0.2 g, 1.9 mmol) were placed in a high-pressure tube filled with argon. Freshly distilled triethylamine (5 cm^3) was cannulated into the tube, and the solution formed was stirred and heated at 70 °C over 20 h. A gray precipitate (Et_3N·HBr) was filtered off and washed with diethyl ether (20 cm^3), and the filtrate was concentrated in vacuo. The thick oil formed was treated with a small amount of petroleum ether, which caused crystallization of the crude product. The product was recrystallized from petroleum ether (60−80 °C). Yield: 0.3 g (85%). Mp: 67−68 °C. IR, ν/cm^{-1}: 3042w, 2231w, 1595s, 1579m, 1560w, 1493m, 1462s, 1422m, 1410m, 1217w, 1141w, 1082w, 989w, 862w, 827m, 778m, 737w, 557w, 509w. ^{1}H NMR ($CDCl_3$, ppm): 8.63−8.70 (m, 3H), 7.74 (t, 1H), 7.59 (d, 1H), 7.48 (d, 2H), 7.33 (dd, 1H). Calc for $C_{12}H_8N_2$: C 80.00, H 4.44, N 15.56. Found: C 79.85, H 4.15, N 15.34. MS (EI, *m*/*z*): 180 $[M]^+$.

2,4′-(4-Ethynylphenyl)bipyridine (2,4′-pyacph). Step 1. 4-(4′-Aminophenyl)pyridine (5 g, 29 mmol) was dissolved in 48% aqueous HBF_4 (23 cm^3) and cooled to −10 °C. To the resulting slurry was added powdered $NaNO_2$ (2.21 g, 32 mmol) at such a rate that no evolution of nitric oxides could be detected. After 30 min, the diazonium salt was filtered off and then added portionwise without delay to a solution of KI (7.83 g, 47 mmol) in an acetone/water (40/60) mixture (50 cm^3). **CAUTION:** diazonium salts are potentially explosive when completely dry. The reaction mixture was then decolorized by adding $Na_2S_2O_3$, neutralized with saturated aqueous Na_2CO_3, and extracted with chloroform (3 × 50 cm^3). The organic layer was dried over $MgSO_4$ and evaporated to yield crude 4-(4′-iodophenyl)pyridine. The crude product was purified by recrystallization from toluene. Yield: 5.07 g (61%). Mp: 204−207 °C. ^{1}H NMR ($CDCl_3$, ppm): 8.68 (d, 2H), 7.84 (d, 2H), 7.48 (d, 2H), 7.39 (d, 2H). MS (EI, *m*/*z*): 281 (M^+).

Step 2. Freshly recrystallized 4-(4′-iodophenyl)pyridine (0.2 g 0.7 mmol), 2-ethynylpyridine (0.1 g 1.0 mmol), $Pd(PPh_3)_4$ (5 mg), $Pd(PPh_3)_2Cl_2$ (10 mg), and copper(I) bromide (5 mg) were placed in a round-bottom flask. The flask was flushed with argon, and dry triethylamine (2 cm^3) was cannulated into the flask. The temperature of the reaction mixture was slowly raised from 20 °C to reflux, and the mixture was then refluxed and stirred for 40 h. The reaction mixture was cooled, and chloroform (5 cm^3) was added to dissolve the solid product. The organic layer was separated and washed with saturated aqueous Na_2CO_3 (10 cm^3) and dried over Na_2SO_4. The chloroform was then evaporated in vacuo, and the crude product was purified by column chromatography (toluene/acetone, 3:1, silicagel-60). Yield: 0.1 g (55%). Mp: 144 °C. IR, ν/cm^{-1}: 2963m, 2925w, 2216w, 1618w, 1592s, 1562m, 1534m, 1501w, 1473m, 1412m, 1384m, 1322m, 1262s, 1215m, 1097s, 864m, 805s, 752m, 700m, 636m. ^{1}H NMR ($CDCl_3$, ppm): 8.71 (br d, 2H), 8.65 (d, 1H), 7.74 (d, 2H), 7.69 (t, 1H), 7.67 (d, 2H), 7.58 (d, 1H), 7.52 (d, 1H) 7.28 (t, 1H). Calc for $C_{18}H_{14}N_2$: C 84.38, H 5.47, N 10.94. Found: C 84.12, H 5.29, N 10.58. MS (EI, *m*/*z*): 256 $[M]^+$.

2,4′-(4-Phenylethynyl)bipyridine (2,4′-pyphac). Step 1. 4-Bromoiodobenzene (0.41 g, 1.4 mmol), 4-ethynylpyridine (0.15 g, 1.5 mmol), $Pd(PPh_3)_2Cl_2$ (7 mg), and copper(I) bromide (4 mg) were placed in a round-bottom flask. The flask was flushed with argon, and di(isopropyl)-amine (2.5 cm^3) was cannulated into the flask. All the reactants were dissolved at room temperature, and 5−10 min later an exothermal reaction spontaneously started (external cooling of the flask with water bath is required in case of excessive heating). The reaction was complete in 30 min, and the solidified mixture of products was dissolved in chloroform (15 cm^3). The organic solution was washed with a saturated aqueous solution of Na_2CO_3 (15 cm^3). The organic layer was dried over Na_2SO_4, and the solvent was evaporated in a vacuum, resulting in analytically pure 4-(4-bromophenylethynyl)pyridine. Yield: 0.36 g (97%). Mp: 142−144 °C. ^{1}H NMR ($CDCl_3$, ppm): 8.63 (d, 2H), 7.54 (d, 2H), 7.42 (d, 2H), 7.38 (d, 2H). MS (EI, *m*/*z*): 177 $[M - Br]^+$, 257 $[M]^+$.

Step 2. 4-(4-Bromophenylethynyl)pyridine (0.72 g, 2.8 mmol), dimethyl-2-pyridylboronate (0.5 g, 3.3 mmol), powdered potassium hydroxide (0.22 g, 3.9 mmol), $Pd(PPh_3)_4$ (0.1 g), and tetraethylammonium bromide (0.05 g) were placed in a high-pressure tube. The tube was flushed with argon, and deoxygenated toluene (30 cm^3) was cannulated in. The resultant solution was stirred and heated at 110 °C over 12 h. The reaction mixture was treated with water (50 cm^3), and the organic products were extracted with dichloromethane (3 × 50 cm^3). The organic layer was washed with water (50 cm^3) and dried over Na_2SO_4. The solvent was removed to give the crude product. The product was purified by column chromatography (toluene/ethyl acetate, 4:1, silicagel-60). Yield: 0.4 g (56%). Mp: 160−161 °C. IR, ν/cm^{-1}: 3026w, 2221m, 1590s, 1571w, 1537w, 1462m, 1433m, 1409m, 1217m, 1014w, 988w, 853m, 824m, 781s, 722w, 685w, 547w, 501w. ^{1}H NMR ($CDCl_3$, ppm): 8.73 (d, 1H), 8.63 (d, 2H), 8.07 (d, 2H), 7.79 (m, 2H),

(18) Champness, N. R.; Khlobystov, A. N.; Majuga, A. G.; Schröder, M.; Zyk, N. V. *Tetrahedron Lett.* **1999**, *40*, 5413.
(19) Ames, D. E.; Bull, D.; Takundwa, C. *Synthesis* **1981**, 364.
(20) Fernando, S. R. L.; Maharoof, U. S. M.; Deshayes, K. D.; Kinste, T. H.; Ogawa, M. Y. *J. Am. Chem. Soc.* **1996**, *118*, 5783.
(21) Singh, B. *Heterocycles* **1984**, *22*, 795.

7.68 (d, 2H), 7.42 (d, 2H), 7.26 (m, 1H). Calc for $C_{18}H_{14}N_2$: C 84.38, H 5.47, N 10.94. Found: C 84.35, H 5.15, N 10.67. MS (EI, *m*/*z*): 256 $[M]^+$.

Complex Synthesis. 1, [Cd(NO$_3$)$_2$(4-phenylpyridine)$_3$](MeCN)$_2$. A solution of $Cd(NO_3)_2 \cdot 4H_2O$ (20 mg, 6.5×10^{-2} mmol) in MeCN (2 cm^3) was layered over a solution of 4-phenylpyridine (30 mg, 19.4×10^{-2} mmol) in dichloromethane (2 cm^3). After 3 days, colorless blocky crystals suitable for X-ray diffraction were formed (yield 35 mg, 77%). IR, ν/cm^{-1}: 3063w, 3034w, 1609s, 1485m, 1449m, 1416m, 1883s, 1371s, 1290m, 1223w, 762m, 731m, 692m, 618m. Calc for $C_{37}H_{33}CdN_7O_6$: C 56.68, H 4.24, N 12.50. Found: C 56.10, H 4.12, N 12.31.

2, [Cd(NO$_3$)$_2$(2,4′-bipy)MeCN]$_2$. A solution of $Cd(NO_3)_2 \cdot 4H_2O$ (15 mg, 4.9×10^{-2} mmol) in MeCN (2 cm^3) was added to a solution of 2,4′-bipy (8 mg, 4.9×10^{-2} mmol) in CH_2Cl_2 (2 cm^3). Slow diffusion of Et_2O vapor into the solution resulted in colorless plate crystals (yield 15 mg, 53%). IR, ν/cm^{-1}: 3050w, 1601s, 1584m, 1565w, 1469m, 1377s, 1312s, 778m, 744m, 511w. Calc for $C_{12}H_{11}CdN_5O_6$: C 33.18, H 2.53, N 16.13. Found: C 32.51, H 2.50, N 15.57. MS (ES, *m*/*z*): 759 $[M - NO_3 + 2H_2O]^+$.

3, [Cd(NO$_3$)$_2$(2,4′-pyph)MeCN]$_2$. A solution of $Cd(NO_3)_2 \cdot 4H_2O$ (11 mg, 3.6×10^{-2} mmol) in MeCN (6 cm^3) was layered over a solution of 2,4′-pyph (8 mg, 3.6×10^{-2} mmol) in a 1:1 (v/v) mixture of CH_2Cl_2 and hexafluorobenzene (2 cm^3). The complex $[Cd(NO_3)_2(2,4'\text{-pyph})MeCN]_2$ is formed as the main product (colorless plate crystals). IR, ν/cm^{-1}: 3114w, 3055w, 1610s, 1589w, 1563w, 1466m, 1436m, 1384s, 1333m, 1232m, 1157w, 1008w, 826m, 784w, 775m, 720m, 611w, 539w. Calc for $C_{18}H_{15}CdN_5O_6$: C 42.35, H 2.94, N 13.73. Found: C 42.11, H 3.01, N 13.55. MS (ES, *m*/*z*): 912 $[M - NO_3 + 2H_2O]^+$.

4, [Cd(NO$_3$)$_2$(2,4′-pyac)DMF]$_2$. A solution of $Cd(NO_3)_2 \cdot 4H_2O$ (15 mg, 4.9×10^{-2} mmol) in MeCN (2 cm^3) was added to a solution of 2,4′-pyac (9 mg, 4.9×10^{-2} mmol) in DMF (2 cm^3). Slow diffusion of Et_2O vapor into the solution resulted in colorless blocky crystals (yield 18 mg, 76%). IR, ν/cm^{-1}: 3444m, 3044w, 2425w, 1655s, 1597s, 1580m, 1563w, 1463m, 1376s, 1299s, 827m, 777m, 744m 557w, 509w. Calc for $C_{15}H_{15}CdN_5O_7$: C 36.73, H 3.06, N 14.29. Found: C 36.00, H 3.20, N 13.55. MS (ES, *m*/*z*): 780 $[M - NO_3 + 2H_2O]^+$.

5, {[Cd(NO$_3$)$_2$(2,4′-pyacph)]MeCN}$_\infty$. A solution of $Cd(NO_3)_2 \cdot 4H_2O$ (12 mg, 3.9×10^{-5} mol) in CH_3CN (2 cm^3) was layered over a solution of 2,4′-pyacph (10 mg, 3.9×10^{-5} mol) in CH_2Cl_2 (2 cm^3). Colorless columnar crystals suitable for X-ray diffraction were formed overnight (yield 35 mg, 93%). IR (ν, cm^{-1}): 2229w, 1615s, 1452s, 1384vs, 1292s, 814w. Calc for $C_{40}H_{30}Cd_2N_{10}O_{12}$: C 45.03, H 2.81, N 13.13. Found: C 45.45, H 2.90, N 12.98. MS (ES/MeOH): *m*/*z* 941 $[M - NO_3 + H_2O]$.

6, {[Cd(NO$_3$)$_2$(2,4′-pyacph)]}$_\infty$. A mixture of $Cd(NO_3)_2 \cdot 4H_2O$ (12 mg, 3.9×10^{-5} mol) and 2,4′-pyacph (10 mg, 3.9×10^{-5} mol) was heated in Bu^{n}OH/*o*-xylene (4 cm^3, 1:1 v/v) at 130 °C for 30 min and then slowly cooled to room temperature. Colorless platy crystals suitable for X-ray diffraction were formed (yield 34 mg, 90%). Complex **5** is quantitatively transformed to **6** when heated in the mother liquor at 130 °C over 1 h. IR (ν, cm^{-1}): 2218w, 1614s, 1467s, 1384vs, 813w. Calc for $C_{36}H_{24}Cd_2N_8O_{12}$: C 43.90, H 2.44, N 11.38. Found: C 43.34, H 2.44, N 11.17. MS (ES/MeOH): *m*/*z* 941 $[M - NO_3 + H_2O]$.

7, {[Cd(NO$_3$)$_2$(2,4′-pyacph)Pr^{i}OH]$_2$}$_\infty$. A solution of $Cd(NO_3)_2 \cdot 4H_2O$ (12 mg, 3.9×10^{-2} mmol) in Pr^{i}OH (2 cm^3) was layered over a solution of 2,4′-pyacph (10 mg, 3.9×10^{-2} mmol) in CH_2Cl_2/toluene (1:1 v/v 2 cm^3). Colorless block-shaped crystals (yield 35 mg, 91%) suitable for X-ray diffraction were formed over 5 days. IR, ν/cm^{-1}: 3400m, 2222w, 1612s, 1492w, 1384vs, 1287w, 815w. Calc $C_{36}H_{24}Cd_2N_8O_{12}$: C 43.90, H 2.44, N 11.38. Found: C 44.03, H 2.67, N 11.09. MS (ES, *m*/*z*): 941 $[M - NO_3^- + H_2O]^+$.

The compound $\{[Cd(NO_3)_2(2,4'\text{-pyacph})(Pr^iOH)]_2\}_\infty$ (**7**) co-crystallized with the complex $\{[Cd(NO_3)_2(2,4'\text{-pyacph})]_2\}_\infty$ (**6**) and then gradually lost Pr^{i}OH, transforming almost completely to **6**.

8, {[Cd(NO$_3$)$_2$(2,4′-pyphac)]}$_\infty$. A mixture of $Cd(NO_3)_2 \cdot 4H_2O$ (12 mg, 3.9×10^{-2}mmol) and 2,4′-pyphac (10 mg, 3.9×10^{-2}mmol) was heated in Bu^{n}OH/*o*-xylene (4 cm^3, 1:1 v/v) at 120 °C for 4 h and then slowly cooled to room temperature. Colorless blocky crystals (yield 36 mg, 96%) suitable for X-ray diffraction were formed. IR, ν/cm^{-1}: 2220s, 1607s, 1462s, 1329s, 1286s, 1220s, 1014m, 831w, 787w. Calc for $C_{36}H_{24}Cd_2N_8O_{12}$: C 43.90, H 2.44, N 11.38. Found: C 43.65, H 2.50, N 11.98. MS (ES, *m*/*z*): 941 $[M - NO_3^- + H_2O]^+$.

9, {[Cd(NO$_3$)$_2$(2,4′-pyphac)$_2$H$_2$O]}$_\infty$. A solution of $Cd(NO_3)_2 \cdot 4H_2O$ (12 mg, 3.9×10^{-2} mmol) in MeCN (2 cm^3) was layered over a solution of 2,4′-pyphac (10 mg, 3.9×10^{-2} mmol) in CH_2Cl_2 (2 cm^3). Colorless plate crystals suitable for X-ray diffraction were formed overnight (yield 33 mg, 90%). IR, ν/cm^{-1}: 2220m, 1607m, 1463m, 1463m, 1384s, 1329w, 1289w, 1220w, 1013w, 831w, 787w. Calc for $C_{36}H_{26}CdN_6O_7$: C 56.32, H 3.39, N 10.95. Found: C 56.35, H 3.30, N 10.59. MS (ES, *m*/*z*): 705 $[M - NO_3 + H_2O]^+$.

The mononuclear complex **9** was irreversibly transformed into the complex $\{[Cd(NO_3)_2(2,4'\text{-pyphac})]_2\}_\infty$ (**8**) when heated in a mixture of Bu^{n}OH/*o*-xylene at 120 °C.

X-ray Crystallography. Single-crystal X-ray experiments were performed on Bruker SMART CCD area detector diffractometers equipped with an Oxford Cryosystems open-flow cryostat using graphite-monochromated Mo Kα radiation ($\lambda = 0.71073$ Å) for compounds **1**, **2**, and **4**−**8** and synchrotron radiation ($\lambda = 0.6942$ Å and $\lambda = 0.6892$ Å for compounds **3** and **9**, respectively). Structures **3** and **5** were solved by heavy atom methods, and structures **1**, **2**, **4**, and **6**−**9** were solved by direct methods;[23] all remaining non-hydrogen atoms were located in difference Fourier syntheses.[24]

Crystal data for **1**: $C_{37}H_{33}CdN_7O_6$, $M_r = 784.10$, triclinic, space group $P\bar{1}$, $a = 12.8471(7)$ Å, $b = 13.0727(7)$ Å, $c = 13.0765(7)$ Å, $\alpha = 113.780(2)°$, $\beta = 95.372(2)°$, $\gamma = 112.184(2)°$, $V = 1780.9(2)$ Å^3.

Crystal data for **2**: $C_{24}H_{22}Cd_2N_{10}O_{12}$, $M_r = 867.32$, triclinic, space group $P\bar{1}$, $a = 7.8735(7)$ Å, $b = 8.1441(7)$ Å, $c = 12.9572(11)$ Å, $\alpha = 78.804(1)°$, $\beta = 78.681(1)°$, $\gamma = 68.581(1)°$, $V = 751.6(2)$ Å^3.

Crystal data for **3**: $C_{36}H_{30}Cd_2N_{10}O_{12}$, $M_r = 1019.52$, triclinic, space group $P\bar{1}$, $a = 8.992(4)$ Å, $b = 10.657(6)$ Å, $c = 10.684(6)$ Å, $\alpha = 77.01(6)°$, $\beta = 74.64(6)°$, $\gamma = 88.29(7)°$, $V = 961.6(9)$ Å^3.

Crystal data for **4**: $C_{30}H_{30}Cd_2N_{10}O_{14}$, $M_r = 979.44$, triclinic, space group $P\bar{1}$, $a = 8.4570(13)$ Å, $b = 9.581(2)$ Å, $c = 12.026(2)$ Å, $\alpha = 88.117(2)°$, $\beta = 88.678(3)°$, $\gamma = 82.132(2)°$, $V = 964.6(3)$ Å^3.

Crystal data for **5**: $C_{40}H_{30}Cd_2N_{10}O_{12}$, $M_r = 1067.54$, monoclinic, space group $C2/c$, $a = 26.583(8)$ Å, $b = 8.143(2)$ Å, $c = 21.270(6)$ Å, $\beta = 117.112(2)°$, $V = 4098(4)$ Å^3.

Crystal data for **6**: $C_{36}H_{24}Cd_2N_8O_{12}$, $M_r = 985.44$, triclinic, space group $P\bar{1}$, $a = 8.3796(9)$ Å, $b = 8.4698(9)$ Å, $c = 12.8983(14)$ Å, $\alpha = 83.743(2)°$, $\beta = 76.014(2)°$, $\gamma = 85.366(2)°$, $V = 881.5(3)$ Å^3.

Crystal data for **7**: $C_{41.6}H_{39.2}Cd_2N_8O_{14.4}$, $M_r = 1106.40$, monoclinic, space group $P2_1/c$, $a = 13.2770(8)$ Å, $b = 13.2606(8)$ Å, $c = 14.3240(8)$ Å, $\beta = 114.656(1)°$, $V = 2292.0(4)$ Å^3.

Crystal data for **8**: $C_{36}H_{24}Cd_2N_8O_{12}$, $M_r = 985.44$, monoclinic, space group $P2_1/c$, $a = 8.5354(8)$ Å, $b = 15.0114(14)$ Å, $c = 14.7187(13)$ Å, $\beta = 99.674(2)°$, $V = 1859.1(5)$ Å^3.

Crystal data for **9**: $C_{36}H_{26}CdN_6O_7$, $M_r = 767.03$, monoclinic, space group Cc, $a = 38.754(8)$ Å, $b = 10.189(2)$ Å, $c = 8.479(2)$ Å, $\beta = 102.13(3)°$, $V = 3273.3(11)$ Å^3.

Crystallographic data (excluding structure factors) for the structures reported in this paper have been deposited with the Cambridge Crystallographic Data Centre as supplementary publication nos. 192297 (**1**), 192298 (**2**), 192299 (**3**), 192300 (**4**), 168544 (**5**), 168543 (**6**), 168545 (**7**), 168546 (**8**), and 192301 (**9**). Copies of the data can be obtained free of charge on application to CCDC, 12 Union Road, Cambridge CB2 1EZ, UK (fax: (+44) 1223-336-033; e-mail: deposit@ccdc.cam.ac.uk).

(22) Coudret, C. *Synth. Commun.* **1996**, 3543.
(23) Sheldrick, G. M. *SHELXS-97. Acta Crystallogr. Sect. A* **1990**, *46*, 467.
(24) Sheldrick, G. M. *SHELXL-97*; Universität Göttingen: Germany, 1997.

Acknowledgment. We thank the EPSRC for support, CLRC for access to Station 9.8 on the Daresbury SRS, the CVCP, and the University of Nottingham for an ORS Award (to A.N.K.). We also thank Mr. Oleg V. Dolomanov for help in topological analysis of the polymeric structures.

Supporting Information Available: X-ray crystallographic data. This material is available free of charge via the Internet at http://pubs.acs.org.

JA029048Y